

# Inflammasome activation in neutrophils of patients with severe COVID-19

Karen Aymonnier,<sup>1-3</sup> Julie Ng,<sup>4</sup> Laura E. Fredenburgh,<sup>4</sup> Katherin Zambrano-Vera,<sup>4</sup> Patrick Münzer,<sup>1-3,5</sup> Sarah Gutch,<sup>1-3</sup> Shoichi Fukui,<sup>1,2</sup> Michael Desjardins,<sup>6,7</sup> Meera Subramaniam,<sup>8</sup> Rebecca M Baron,<sup>4</sup> Benjamin A. Raby,<sup>9</sup> Mark A. Perrella,<sup>4,10</sup> James A. Lederer,<sup>11</sup> and Denisa D. Wagner<sup>1-3,12</sup>

<sup>1</sup>Program in Cellular and Molecular Medicine, Boston Children's Hospital, Boston, MA; <sup>2</sup>Department of Pediatrics, Harvard Medical School, Boston, MA; <sup>3</sup>Whitman Center, Marine Biological Laboratory, Woods Hole, MA; <sup>4</sup>Division of Pulmonary and Critical Care Medicine, Department of Medicine, Brigham and Women's Hospital and Harvard Medical School, Boston, MA; <sup>5</sup>Department of Cardiology and Angiology, University of Tübingen, Tübingen, Germany; <sup>6</sup>Department of Medicine, Brigham and Women's Hospital, Boston, MA; <sup>7</sup>Division of Infectious Diseases, Centre Hospitalier de l'Université de Montréal, Montreal, Quebec, Canada; <sup>8</sup>Division of Pulmonary Medicine, and <sup>9</sup>Division of Pulmonary Medicine, Department of Pediatrics, Boston Children's Hospital, Boston, MA; <sup>10</sup>Department of Pediatric Newborn Medicine, and <sup>11</sup>Department of Surgery, Brigham and Women's Hospital and Harvard Medical School, Boston, MA; and <sup>12</sup>Division of Hematology/Oncology, Boston Children's Hospital, Boston, MA

## Key Points

- Neutrophils with intact multilobulated nuclei show ASC speck formation and high histone H3 citrullination in patients with severe COVID-19.
- In murine neutrophils, ASC speck forms transiently at the microtubule organizing center, before nuclear rounding, early in NETosis.

Infection by the severe acute respiratory syndrome coronavirus 2 (SARS-CoV-2) engages the inflammasome in monocytes and macrophages and leads to the cytokine storm in COVID-19. Neutrophils, the most abundant leukocytes, release neutrophil extracellular traps (NETs), which have been implicated in the pathogenesis of COVID-19. Our recent study shows that activation of the NLRP3 inflammasome is important for NET release in sterile inflammation. However, the role of neutrophil inflammasome formation in human disease is unknown. We hypothesized that SARS-CoV-2 infection may induce inflammasome activation in neutrophils. We also aimed to assess the localization of inflammasome formation (ie, apoptosis-associated speck-like protein containing a CARD [ASC] speck assembly) and timing relative to NETosis in stimulated neutrophils by real-time video microscopy. Neutrophils isolated from severe COVID-19 patients demonstrated that ~2% of neutrophils in both the peripheral blood and tracheal aspirates presented ASC speck. ASC speck was observed in neutrophils with an intact poly-lobulated nucleus, suggesting early formation during neutrophil activation. Additionally, 40% of nuclei were positive for citrullinated histone H3, and there was a significant correlation between speck formation and nuclear histone citrullination. Time-lapse microscopy in lipopolysaccharide -stimulated neutrophils from fluorescent ASC reporter mice showed that ASC speck formed transiently and at the microtubule organizing center long before NET release. Our study shows that ASC speck is present in neutrophils from COVID-19 patients with respiratory failure and that it forms early in NETosis. Our findings suggest that inhibition of neutrophil inflammasomes may be beneficial in COVID-19.

## Introduction

The coronavirus disease 2019 (COVID-19) pandemic caused by the severe acute respiratory syndrome coronavirus 2 (SARS-CoV-2) is clinically heterogenous, ranging from mild flu-like symptoms to acute respiratory distress syndrome and sometimes progressing to multisystem organ failure.<sup>1</sup> Severe COVID-19 is

Submitted 16 August 2021; accepted 12 December 2021; prepublished online on *Blood Advances* First Edition 6 January 2022; final version published online 28 March 2022. DOI 10.1182/bloodadvances.2021005949.

Any original datasets and protocols can be available to other investigators. Requests for data sharing may be submitted to Karen Aymonnier (aymonnier.karen@hotmail.fr).

The full-text version of this article contains a data supplement.

Licensed under Creative Commons Attribution-NonCommercial-NoDerivatives 4.0 International (CC BY-NC-ND 4.0), permitting only noncommercial, nonderivative use with attribution. All other rights reserved.

associated with an overly exuberant inflammatory response, including hyperactivation of immune cells and elevated levels of proinflammatory cytokines in the blood.<sup>2,3</sup> For example, high levels of interleukin (IL)-1 $\beta$  and IL-6 were detected in lung autopsies and plasma from SARS-CoV-2 infected patients.<sup>2,4</sup> Additionally, an increased percentage of IL-1 $\beta$ -producing monocytes has been detected in the blood of COVID-19 patients by single-cell RNA sequencing analysis.<sup>5</sup> Indeed, monocytes and macrophages have been extensively described as the main source of these proinflammatory mediators driving COVID-19 pathology.

Processing of the IL-1 $\beta$  cytokine, a master regulator of inflammation, occurs mostly within inflammasomes. Inflammasomes are intracellular multiprotein signaling platforms that mediate pivotal innate inflammatory responses. Several recent studies using *in vitro* models and clinical samples have shown that SARS-CoV-2 engages inflammasomes and pyroptosis in human monocytes.<sup>6,7</sup> Activation and assembly of the inflammasome activates caspase-1, which cleaves specific proinflammatory cytokines (eg, IL-1 $\beta$ ) into their mature, secreted forms and initiates death by pyroptosis. Inflammasomes can be assembled by select pattern recognition receptors. Apoptosis-associated speck-like protein containing a CARD (ASC) (caspase activation and recruitment domain) is an adaptor molecule composed of an N-terminal pyrin domain and a CARD, which interacts directly with multiple pattern recognition receptors, such as NLRPs (nucleotide-binding oligomerization domain, leucine-rich repeat [NLR] and pyrin domain containing proteins), NLR caspase recruitment domain-containing protein (NLRC), and AIM2 to form an active inflammasome. ASC accumulation at the inflammasome promotes caspase 1 autoactivation. The active inflammasome can be visualized by light microscopy by what is colloquially referred to as a “speck,” a large protein complex decorated by ASC proteins. In activated cells, an ASC speck reaches a size of  $\sim 1 \mu\text{m}$ , and most commonly, only 1 speck per cell forms upon stimulation.<sup>8</sup>

Traditionally, inflammasomes have mainly been studied in monocytes and macrophages, with very little interest in neutrophils. For example, in COVID-19 patients, Rodrigues et al reported that peripheral blood mononuclear cells (PBMCs) demonstrate clear visualization of NLRP3 and ASC speck.<sup>7</sup> However, neutrophils, despite their high numbers, were not examined. Neutrophils constitute the first line of defense against pathogens and are an early responder to stimuli that lead to tissue injury. During injury or infection, activated neutrophils release decondensed DNA and histones from their nucleus, forming a network of extracellular chromatin known as neutrophil extracellular traps (NETs). The intracellular process of forming NETs is called NETosis. A very important step in NETosis is chromatin decondensation initiated by activation of the enzyme peptidyl arginine deiminase 4 (PAD4), which leads to citrullination of histones in the nucleus, thus reducing their positive charge. Citrullinated histones are a good biomarker of NETosis.<sup>9</sup> Although NETosis was initially described to be induced by infection, it also prominently occurs in sterile inflammation. Recently, our team has shown that NLRP3 inflammasome assembly and activation plays an important role in the release of NETs from neutrophils under sterile conditions.<sup>10</sup> In particular, NLRP3 supported both nuclear envelope and plasma membrane rupture during NETosis. Pharmacological inhibition of NLRP3 in either mouse or human neutrophils reduces NETosis.<sup>10</sup>

The pathogenic role of NETs has been demonstrated in a variety of conditions including thrombosis, cancer, ischemia-reperfusion injury,

organ fibrosis, and acute lung injury.<sup>9,11</sup> In animal models of severe ARDS, such as transfusion-related acute lung injury, NETs are extremely damaging, which interferes with blood oxygenation.<sup>12</sup> Interestingly, NETs may play an important role in COVID-19.<sup>13</sup> High blood neutrophil levels are an early indicator of SARS-CoV-2 infection<sup>14</sup> and may cause serious respiratory problems.<sup>15</sup> The excessive accumulation of neutrophils and NETs in the SARS-CoV-2 infected lung may contribute to increased mucous viscosity, which in turn may impair ventilation.<sup>16</sup>

Because NETosis involves inflammasome assembly in sterile inflammation, we hypothesized that inflammasomes may also form in neutrophils during SARS-CoV-2 infection. Together with resulting NETs, neutrophil inflammasome may contribute to severe COVID-19 pathology. In this report, we studied freshly isolated neutrophils from COVID-19 patients. We found the presence of ASC speck in neutrophils from blood and tracheal aspirates and observed high levels of citrullinated nuclei, indicating NETosis. Additionally, using a genetically modified mouse model, we showed that speck forms early in the process of NETosis, thus substantiating the hypothesis that inflammasome regulates NETosis.

## Materials and methods

### Patients

This study was approved by the Institutional Review Boards of Boston Children's Hospital and Brigham and Women's Hospital. Informed consent was obtained from the legally authorized representative or surrogate of eligible COVID-19 patients prior to study participation. Six intensive care unit patients over 18 years of age with COVID-19 pneumonia complicated by respiratory failure requiring intubation and mechanical ventilation were enrolled from 12/9/20 to 1/18/21. Subjects had reverse transcription polymerase chain reaction-confirmed SARS-CoV-2 infection and were enrolled within 120 hours of initiation of mechanical ventilation. A 10 mL ethylenediaminetetraacetic acid (EDTA) blood sample was processed within 1 hour of collection. Demographics and clinical data are summarized in supplemental Table 1.

Aged-matched healthy donor samples were processed and analyzed in parallel with patient samples according to the same protocol. The experimental procedure was approved by the Office of Clinical Investigations at Boston Children's Hospital (protocol number IRB-P00003283). Informed consent was provided by donors.

### Plasma, PBMC, and neutrophils isolation

Ten milliliters of peripheral blood were collected from patients via indwelling venous catheters and from healthy controls by venipuncture in EDTA tubes. Seven milliliters were centrifuged for 10 minutes at  $450 \times g$  for plasma separation. Three milliliters of whole blood were layered over 2 different density Histopaque gradients (Sigma) and centrifuged for 30 minutes at  $872 \times g$ . PBMCs were obtained from the first layer (on Histopaque 1077), and neutrophils were isolated from the second buffy coat layer (on Histopaque 1119). Cells were then washed twice with RPMI without phenol red (Gibco) at  $200 \times g$  for 10 minutes before being quantified. Neutrophils obtained from COVID-19 patients or healthy controls were incubated with RPMI 1640 supplemented with 10 mM *N*-2-hydroxyethylpiperazine-*N'*-2-ethanesulfonic acid (HEPES). Neutrophils and PMBC were attached to slides for 30 minutes at 37°C before

fixation with 4% paraformaldehyde (PFA) for 30 minutes at room temperature (RT) prior to staining.

Healthy human neutrophils attached to the slides were also stimulated as indicated at 37°C, 5% CO<sub>2</sub> with 5 µg/mL lipopolysaccharide (LPS) (from *Klebsiella pneumoniae*, Sigma-Aldrich, cat. L1519) before fixation with 4% PFA for 30 minutes at RT.

### IL-1β measurement in supernatant

Neutrophils from healthy humans were plated at 5 × 10<sup>6</sup> cells per mL in 48-well plates and stimulated with 5 µg/mL LPS (from *K pneumoniae*, Sigma-Aldrich, cat. L1519) for 4 hours at 37°C, 5% CO<sub>2</sub>. Culture supernatants were collected and nonadherent cells removed by centrifugation. Concentration of supernatants was done with Amicon Ultra-0.5 Centrifugal Filter Unit (Millipore) per manufacturer's protocol. IL-1β was measured by enzyme-linked immunosorbent assay according to the manufacturer's instructions (ELISA MAX Deluxe Set Human IL-1β, Biolegend).

### Tracheal aspirates

Tracheal aspirate was obtained from COVID-19 by aspiration of the endotracheal tube. The collected fluids were mixed 1:1 with 0.1 M dithiothreitol (Thermo Fisher Scientific), incubated for 10 minutes at RT, and centrifuged at 400 × g at RT for 10 minutes. Tracheal smears were performed on glass slides and fixed with 4% PFA for 1 hour prior to immunostaining.

### Immunofluorescence

Fixed cells were washed once with phosphate-buffered saline (PBS), permeabilized for 10 minutes at 4°C, and incubated with blocking buffer (2.5% bovine serum albumin, 0.5% Tween-20 in 1 × PBS) at 37°C for 1 hour. Afterward, the samples were incubated at 4°C overnight with the following primary antibodies: rabbit anti-citrullinated histone H3 (1:500; Abcam, cat. ab5103), rabbit anti-ASC (1:400; Adipogen, clone AL177), mouse anti-CD66b (1:500; Biolegend cat. 305102). The samples were washed in PBS and incubated with secondary antibodies: donkey anti-mouse immunoglobulin G AlexaFluor 555 (1:1500; Thermo Fisher Scientific, cat. A32787, 1:1500) or donkey anti-rabbit AlexaFluor 488 (1:1500, Abcam, cat. ab150061). After another 3 wash steps with PBS, the samples were mounted using mounting medium containing 4',6-diamidin-2-phenylindole (DAPI). Images were visualized on an Axiovert 200M wide-field fluorescence microscope (Zeiss) coupled to an AxioCam MR3 monochromatic CCD camera (Zeiss) using a Zeiss Plan-Apochromat 63×/1.4 oil differential interference contrast (DIC) objective lens with the Zeiss AxioVision software (version 4.6.3.0). Images were identically acquired and processed with Fiji/imageJ software.

For confocal microscopy, imaging of immunostainings was carried out on a Zeiss LSM 780 confocal microscope with a 100× oil objective.

### Mice

C57BL/6 mice and R26-CAG-ASC-citrine mice [B6.Cg-Gt(ROSA)26Sortm1.1(CAG-Pycard/mCitrine\*, -CD2\*)Dtg/J] were acquired from The Jackson Laboratory (stock no. 000664 and 030744) and were crossed to obtain heterozygous R26-CAG-ASC-citrine mice in the animal facility of Boston Children's Hospital. All experimental animal procedures in this study were approved by the

Institutional Animal Care and Use Committee of Boston Children's Hospital under the protocol number 20-06-4140R.

### Isolation of murine neutrophils

Murine neutrophils were freshly isolated from the blood of heterozygous ASC reporter mice. Mice were bled for 1 mL via the retro-orbital plexus into 2 mL anticoagulant (15 mM EDTA and 1% bovine serum albumin in sterile PBS) after being deeply anesthetized with isoflurane. The blood was centrifuged at 500 × g for 12 minutes at room temperature. The supernatant was removed, and cells were resuspended in anticoagulant before loaded on top of a Percoll gradient column of 52%/69%/78% in a 15 mL centrifuge tube. The column was then centrifuged at 1500 × g for 32 minutes at RT with acceleration set at 3 and deceleration set at 0. Cells at the 69%/78% interface were collected and pelleted with addition of PBS at 500 × g for 12 minutes at room temperature. After lysis of red blood cells with water, neutrophils were then resuspended in imaging media (phenol red-free RPMI 1640 supplemented with 10 mM *N*-2-hydroxyethylpiperazine-*N'*-2-ethanesulfonic acid, either stained with silicon rhodamine (SiR)-DNA or SiR-tubulin (Cytoskeleton) according to the manufacturers' directions for immediate live imaging and stimulated for NETosis.

### Time-lapse visualization by spinning disc confocal and DIC microscopy

Time-lapse microscopy was performed using isolated peripheral neutrophils from R26-ASC-citrine reporter mice. After staining, cells were washed and resuspended in 300 µL of imaging media before the cell suspension was added and allowed to adhere for 5 minutes in a non-coated 24-well glass bottom plate located on a 37°C prewarmed microscope stage. Three to 10 random fields per well were visualized using a Nikon Eclipse Ti2 microscope equipped with Perfect Focus, a Yokogawa CSU-W1 spinning disc scanhead, a Nikon motorized stage with xy linear encoders containing a Nano-Z100 piezo insert, and a Hamamatsu Orca-flash 4.0 v3 camera with a Plan Apo TIRF 60× oil 1.49 NA DIC Nikon objective lens. Confocal and DIC images were acquired every 2 minutes for the first 60 minutes and every 5 minutes for the rest of the visualization, up to 4 hours. After imaging the baseline for 3 cycles (6 minutes), 300 µL of imaging medium containing LPS (from *K pneumoniae*, Sigma-Aldrich, cat. L1519) was added to achieve a final LPS concentration of 10 µg/mL.

### Statistical analyses

Statistical analysis of differences between groups was performed using the appropriate test as indicated. A *P* value less than .05 was considered significant.

## Results

Six patients with SARS-COV-2 infection diagnosed by nasopharyngeal reverse transcription polymerase chain reaction were enrolled in this study. All subjects were admitted to the intensive care unit for COVID-19 pneumonia complicated by respiratory failure requiring intubation and mechanical ventilation. Demographic and clinical characteristics are shown in supplemental Table 1 and supplemental Figure 1. First, we assessed cleaved mature IL-18 and IL-1β in plasma from COVID-19 patients and compared them with plasma from 8 age-matched healthy controls (Figure 1A-B; supplemental Figure 1A) as downstream readouts for inflammasome activation. In

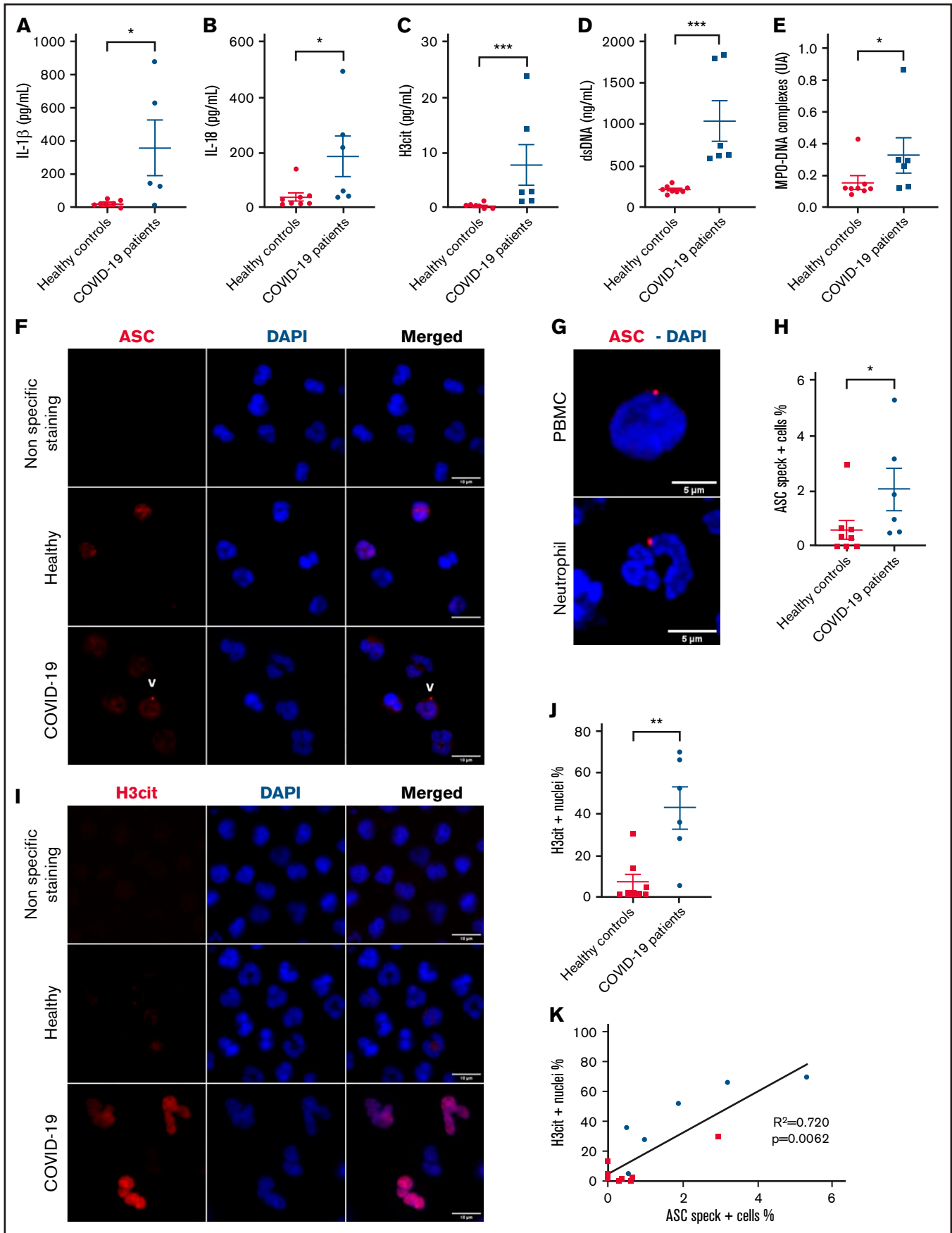


Figure 1.

concordance with literature, we found significantly higher concentrations of IL-1 $\beta$  and IL-18 in the plasma of COVID-19 patients compared with the healthy controls (Figure 1A-B), suggesting the presence of an active inflammasome in these patients. As others before us,<sup>15</sup> we observed a highly significant increase in plasma levels of NET biomarkers H3cit, DNA-myeloperoxidase complexes, and double-stranded DNA (Figure 1C-E).

### Circulating neutrophils from severe COVID-19 patients form ASC speck and begin the process of NETosis, as seen by the presence of H3cit in nuclei

The presence of an inflammasome was recently detected in PBMCs in COVID-19.<sup>7</sup> To decipher if neutrophils can also activate inflammasomes in severe COVID-19, neutrophil and PBMC isolation was initiated within 1 hour of blood drawing. We assessed inflammasome activation by performing immunofluorescence staining of ASC protein. Microscopy revealed the presence of ASC speck (red) in neutrophils (Figure 1F) and confirmed in monocytes (Figure 1G), indicating inflammasome assembly in both of these innate immune cells from COVID-19 patients. Notably, ASC speck was observed in neutrophils with a characteristic multilobulated nucleus and in the usual perinuclear position (Figure 1G). Quantification showed that COVID-19 neutrophils had a significantly higher percentage of ASC speck-positive cells compared with healthy controls (Figure 1H).

We have recently found that the formation of the NLRP3 inflammasome in sterile inflammation is necessary for efficient production of NETs.<sup>10</sup> The citrullinating enzyme PAD4 is also activated during NETosis. Thus, we evaluated neutrophil nuclei for the presence of ongoing citrullination. Not surprisingly, immunofluorescence staining for H3cit in the nuclei was very prominent in ~40% of neutrophils (Figure 1I-J). Remarkably, the percent of ASC speck in neutrophils was significantly correlated with the percent of H3cit positive neutrophil nuclei (Figure 1K), suggesting a link between inflammasome activation and NETosis also after infectious agent-induced stimulation.

### PBMCs from severe COVID-19 patients form ASC speck at similar frequency to neutrophils

ASC speck formation was also assessed quantitatively in fresh PBMCs. The PBMC fraction is mostly composed of lymphocytes and monocytes but can include low density neutrophils (LDNs).<sup>17</sup> Schulte-Schrepping et al reported that LDNs in severe COVID-19 contained immature neutrophils, including pro- and preneutrophils, which was not observed in mild cases of COVID-19.<sup>18</sup> Consequently, specific staining for neutrophils with an anti-CD66b antibody was performed in addition to ASC protein staining (Figure 2A). Our results confirmed a larger subset of LDNs present in the PBMC

fraction of severe COVID-19 (Figure 2B), and most of their nuclei were also positive for H3cit (Figure 2C-E). Similar to Rodrigues et al, we observed a higher percentage of ASC speck-positive cells in the CD66b<sup>-</sup> population of PBMCs in COVID-19 patients compared with healthy controls (Figure 2D). Furthermore, this percentage of cells forming speck was similar to that of neutrophils, ~2%.

### Neutrophils recruited to the lungs in COVID-19-severe patients present inflammasome activation and nuclear citrullination indicative of NETosis

Investigation of myeloid populations present in tracheal aspirates of severe COVID-19 patients showed that granulocytes represent up to 80% of total CD45<sup>+</sup> lung infiltrates.<sup>19</sup> In smears of tracheal aspirates of our patients, we observed that ~60% of the recruited cells were positive for CD66b, indicating a prominent presence of neutrophils (Figure 3A-B). In concordance with peripheral blood neutrophils, ASC specks were detected in neutrophils of tracheal aspirates from COVID-19 patients (Figure 3A and C). Moreover, ~40% of CD66b<sup>+</sup> cells were also positive for H3Cit (Figure 3D). This result explains several prior studies showing that NETs are highly produced in COVID-19 tracheal aspirates.<sup>15</sup> Given that neutrophils are the overwhelming majority (79% to 94%) of the leukocytes in COVID-19 (supplemental Table 1) and ~10 times more prevalent than monocytes in our patients (supplemental Figure 1B), these findings reveal that neutrophils may contribute to cytokine production and pyroptosis via inflammasome activation in the COVID-19 lung and blood. Considering the low sample number, we were not able to find a statistically significant correlation between speck and H3Cit<sup>+</sup> nuclei in neutrophils in tracheal aspirates, although a strong trend toward correlation was noted (Figure 3E).

### Inflammasome assembles early in LPS-stimulated human neutrophils during NETosis

We observed speck mainly in neutrophils from COVID-19 patients with multilobular intact nuclei (Figure 1F-H), suggesting an early inflammasome formation during activation of neutrophils. We studied the *in vitro* time course of ASC speck formation in human neutrophils in response to *K pneumoniae* LPS activation to mimic infection. The quantification of speck formation over time showed that by 1 hour of LPS activation, the number of specks increased, whereas at 4 hours, it was lower and similar to unstimulated neutrophils (Figure 4A and B). NETosis appeared after the formation of speck, typically peaking around 4 hours. Secretion of IL-1 $\beta$  in supernatant was measured at 4 hours and was far higher after LPS activation (Figure 4C). These results suggest that during infection, human neutrophils can trigger speck formation and secretion of IL-1 $\beta$ .

**Figure 1. Circulating neutrophils from COVID-19 pneumonia patients demonstrate inflammasome activation and high nuclear citrullination.** Plasma samples from healthy controls (n = 8) and patients with severe COVID-19 (n = 6) were evaluated for: (A) IL-1 $\beta$ , (B) IL-18, (C) H3cit, (D) dsDNA, and (E) MPO-DNA complexes. Values are means plus or minus SEM. Data were analyzed using Mann-Whitney *U* test; \**P* < .05, \*\*\**P* < .0001. Neutrophils freshly isolated from healthy controls and patients with severe COVID-19 were stained with DAPI (blue) and (F) an anti-ASC antibody (red) or (I) with an anti-H3cit antibody (red). White arrows indicate the presence of the ASC speck. Nonspecific staining corresponds to immunostaining performed without primary antibodies. (F) Representative images from widefield microscopy of neutrophils. Scale bar, 10  $\mu$ m. (G) Representative confocal microscopy images of an immunostained neutrophil and a PBMC from COVID-19 patient. Blue, DNA (DAPI); red, ASC antibody staining. Scale bar, 5  $\mu$ m. (H) Quantification of neutrophils presenting a speck. (I) Representative images from widefield microscopy of neutrophils. Scale bar, 10  $\mu$ m. (J) Quantification of neutrophils with nucleus positive for H3cit. Each dot represents 1 individual. Values are means plus or minus SEM. Data were analyzed by Mann-Whitney *U* test; \**P* < .005, \*\**P* < .001. (K) Correlation between the percentage of neutrophils positive for H3cit and percentage of neutrophils forming speck among all individuals healthy (■) and COVID-19 patients (●). A nonparametric Spearman correlation test was computed. dsDNA, double-stranded DNA; H3cit, citrullinated histone H3; MPO-DNA, myeloperoxidase-DNA; SEM, standard error of the mean.

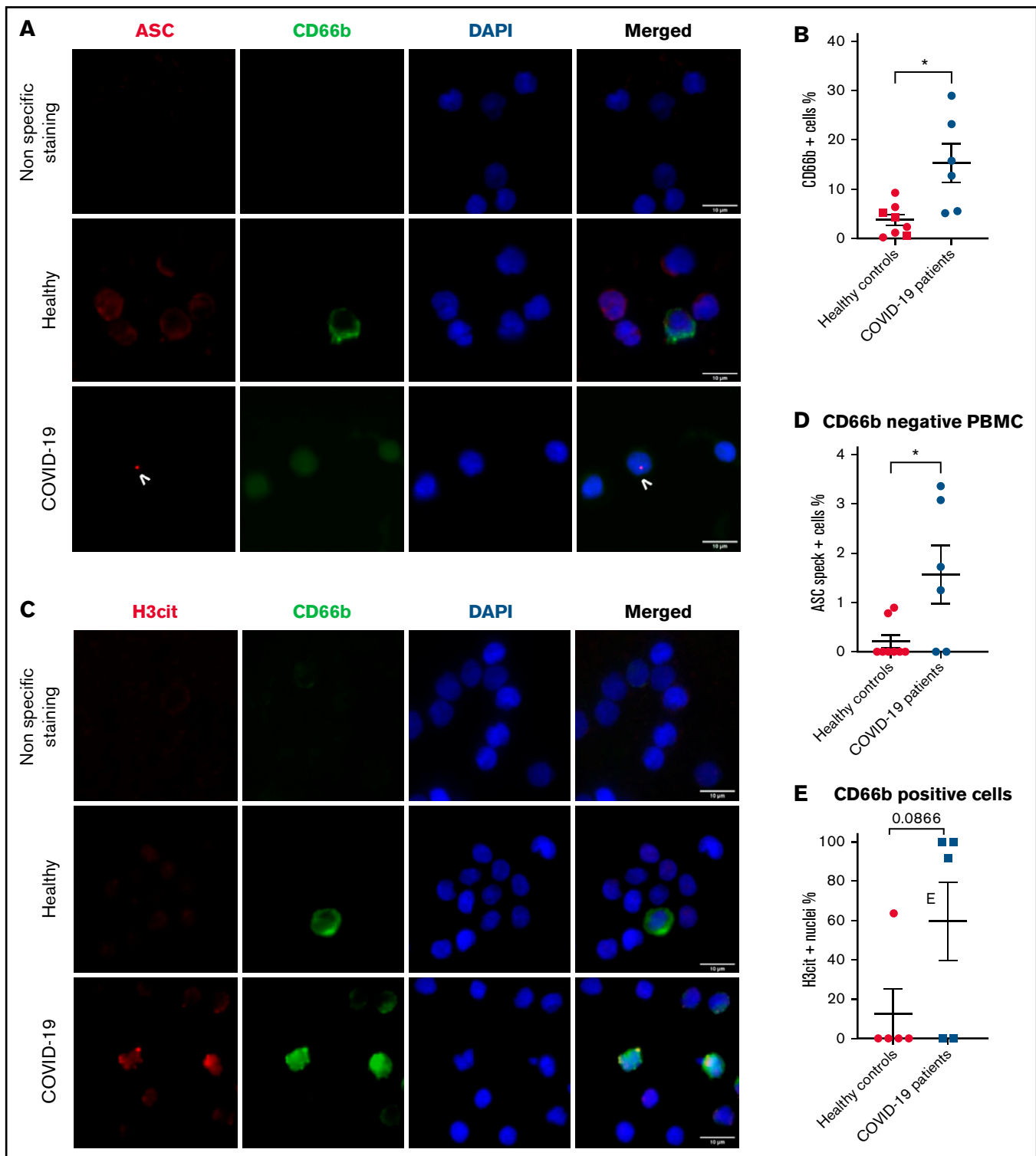


**Figure 2. PBMCs from severe COVID-19 patients form ASC speck at similar frequency to neutrophils.** PBMCs were stained with DAPI (blue), an anti-CD66b antibody (neutrophil marker, green) and (A) an anti-ASC antibody (red), or (C) with an anti-H3cit antibody (red). (A) Representative images from widefield microscopy of PBMCs. Scale bar, 10  $\mu$ m. (B) Quantification of CD66b<sup>+</sup> cells (neutrophils) in PBMC fraction. (C) Representative images from widefield microscopy of PBMCs. Scale bar, 10  $\mu$ m. (D) Quantification of CD66b<sup>-</sup> cells presenting a speck. (E) Quantification of CD66b<sup>+</sup> cells (neutrophils) with nucleus positive for H3cit. Each dot represents 1 individual. Values are means plus or minus SEM. Data were analyzed by Mann-Whitney *U* test; \**P* < .05. SEM, standard error of the mean.

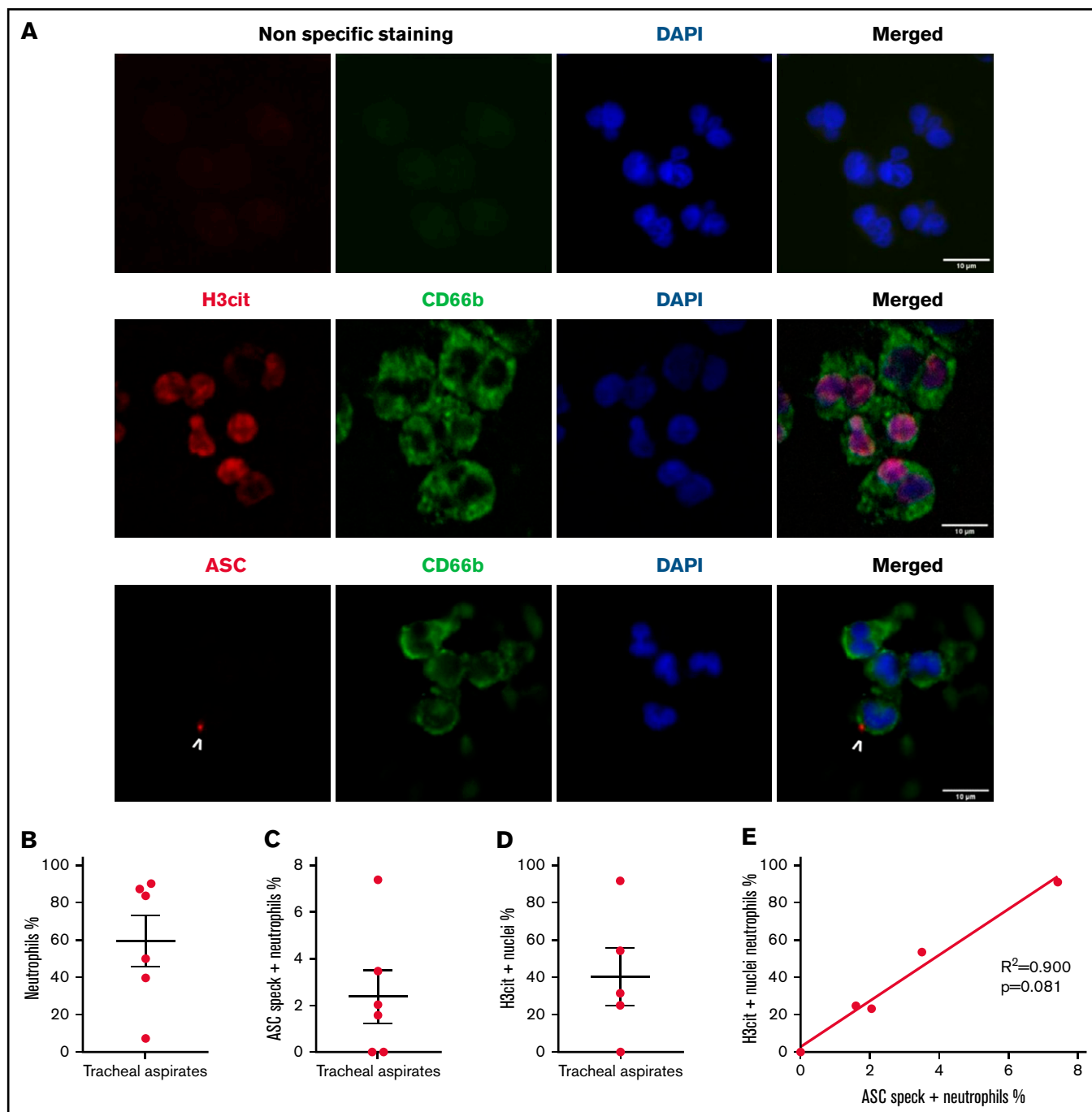


**Figure 3. Neutrophils recruited to the lung in patients with COVID-19 pneumonia have inflammasome activation and are predisposed to NETosis.** Smears of tracheal aspirates were costained with DAPI (blue), an anti-CD66b antibody (neutrophil marker, green) and an anti-ASC antibody (red), or with an anti-H3cit antibody (red). Nonspecific staining corresponds to immunostaining performed without primary antibodies. (A) Representative images from widefield microscopy of tracheal aspirates from severe COVID-19 patients. White arrows indicate the presence of the ASC speck. Scale bar, 10  $\mu$ m. (B) Quantification of CD66b<sup>+</sup> neutrophils in tracheal aspirates. (C) Quantification of ASC speck-positive neutrophils in tracheal aspirates. (D) Quantification of H3cit<sup>+</sup> neutrophils in tracheal aspirates. (E) A nonparametric Spearman correlation test was computed. SEM, standard error of the mean.

### Inflammasome activation occurs transiently near the microtubule-organizing center early during NETosis in LPS-stimulated murine neutrophils

This prompted us to hypothesize that the inflammasome forms early in the process of NETosis before nuclear rounding, thus possibly

regulating NETosis in COVID-19. NETosis comprises a well-orchestrated sequence of cellular events, including loss of cytoplasmic organization, nuclear rounding and swelling, nuclear envelope disassembly, and plasma membrane rupture.<sup>20</sup> The combination of our previous analysis of speck in solely sterile inflammation and the notion that the timing and formation of ASC speck in neutrophils

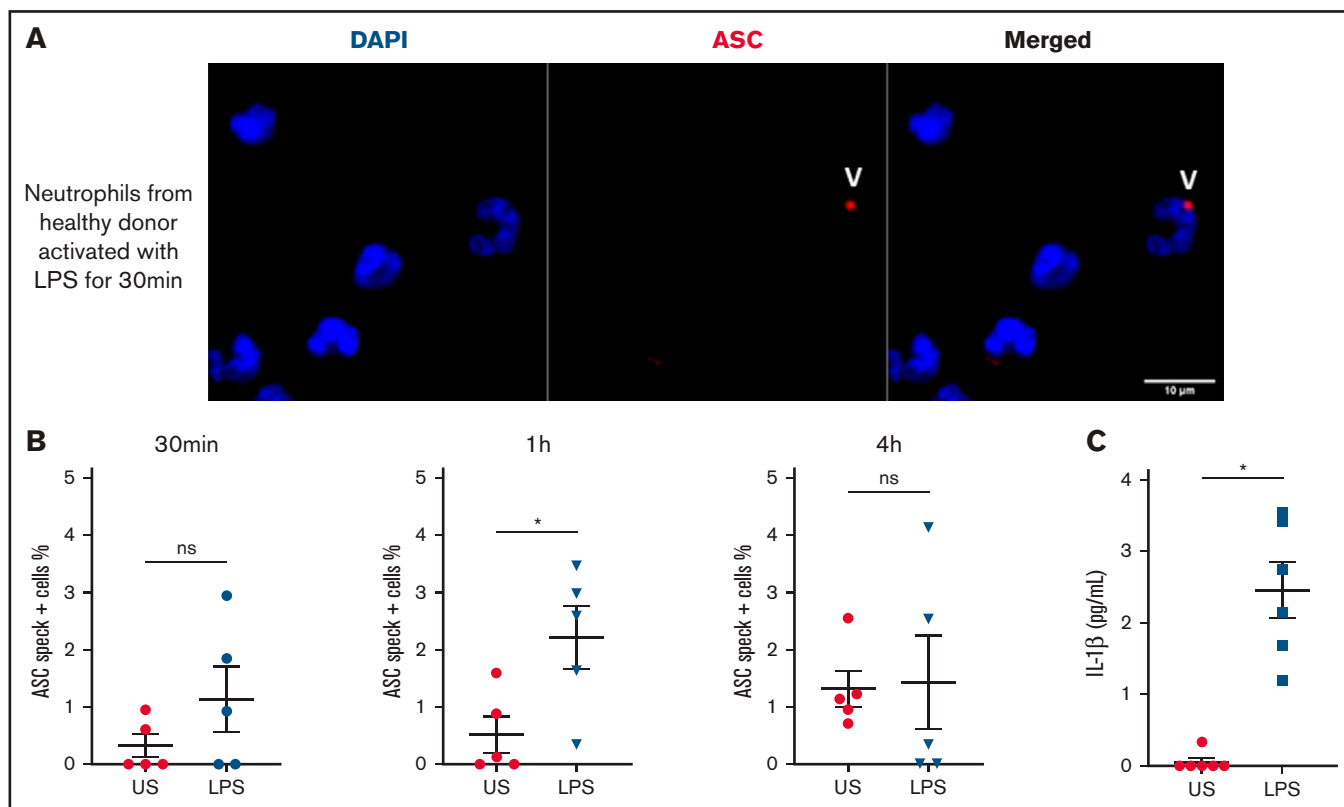


**Figure 4. Human neutrophils activate inflammasome early after LPS activation.** Neutrophils isolated from healthy individuals ( $n = 5$ ) were activated for different lengths of time with  $5 \mu\text{g/mL}$  of LPS and stained with DAPI (blue) and an anti-ASC antibody (red). (A) Representative images from widefield microscopy of neutrophils activated for 30 minutes with  $5 \mu\text{g/mL}$  of LPS. White arrows indicate the presence of the ASC speck. Scale bar,  $10 \mu\text{m}$ . (B) Quantification of neutrophils presenting a speck at 30 minutes, 1 hour, and 4 hours after LPS activation. (C) IL-1 $\beta$  concentration measured in the supernatant of unstimulated (US) neutrophils or activated with LPS. Each dot represents 1 individual. Values are means plus or minus SEM. Data were analyzed by Mann-Whitney  $U$  test;  $*P < .05$ . SEM, standard error of the mean

was not previously described encouraged us to study in details the kinetics and localization of ASC speck during NETosis in mouse neutrophils in real time upon *K pneumoniae* LPS stimulation. We took advantage of transgenic mice that ectopically express the fluorescent adaptor protein ASC-citrine to visualize speck formation and follow the distribution of ASC-associated fluorescence.<sup>21</sup> Cells were stained with the DNA-specific vital dye, SiR-DNA, and DIC and spinning-disk confocal images were acquired at each 2- to 5-minute time interval for 4 hours (Figure 5; videos available online). As described by Thiam, Wong, and colleagues,<sup>20</sup> cells rapidly formed plasma MV upon activation, which is a hallmark of cellular entry into NETosis, and this event was used as an easily visualized temporal initiation point for our study. In brief, MV shedding is followed by nuclear rounding, nuclear rupture with DNA release into the cytoplasm, and finally extracellular DNA expulsion.

Our time lapse videos showed that after LPS stimulation, even before vesiculation, a speck is formed near the nucleus (supplemental Video 1) ~5 minutes before MV shedding (Figure 5A-B). Rounding of the nucleus in LPS-activated cells happened on average at 23 minutes (Figure 5B; supplemental Table 2). Interestingly, the observed ASC speck disappeared in majority of cells before NET formation (supplemental Video 1; Figure 5A-B; supplemental Table 2). The peak number of cells presenting a speck is reached at ~54 minutes after the addition of LPS (Figure 5C). The fluorescence intensity associated with ASC speck was quantified according to time relative to MV

shedding (Figure 5D). Our videos show that high ASC speck fluorescence intensity persists for a minimum of several minutes before showing signs of slow dissolution, remaining visible on average for 80 minutes. This finding suggests a very well-organized spatiotemporal system of inflammasome assembly and disassembly in neutrophils. Speck disappearance was relatively close in time to NETosis (supplemental Table 2; Figure 5B). In the presence of LPS, 54.9% of ASC speck-positive neutrophils completed NETosis, as opposed to only 17.5% of cells in which we did not detect a speck (Figure 5E). This further indicates a functional link between speck and NETosis.

Because MT and microtubules organizing center (MTOC) are important in speck formation in monocytes,<sup>22-24</sup> we analyzed MT dynamics in neutrophils stained with SiR-tubulin (Figure 5F; supplemental Table 2 and Video 2). We observed that ASC speck was assembled in 56% of cells near the MTOC and mostly colocalized with MTs radiating from the MTOC (supplemental Video 2; Figure 5F). Interestingly, under LPS activation, the formation of speck precedes MT disassembly (supplemental Table 2; Figure 5F). Our results clearly indicate that ASC speck is transiently formed at the MTOC near nuclei very early following neutrophil activation and precedes known cellular events of NET formation.

## Discussion

Our clinical study shows that in COVID-19 infection, ASC speck is formed in neutrophils, and the percentage of neutrophils showing a

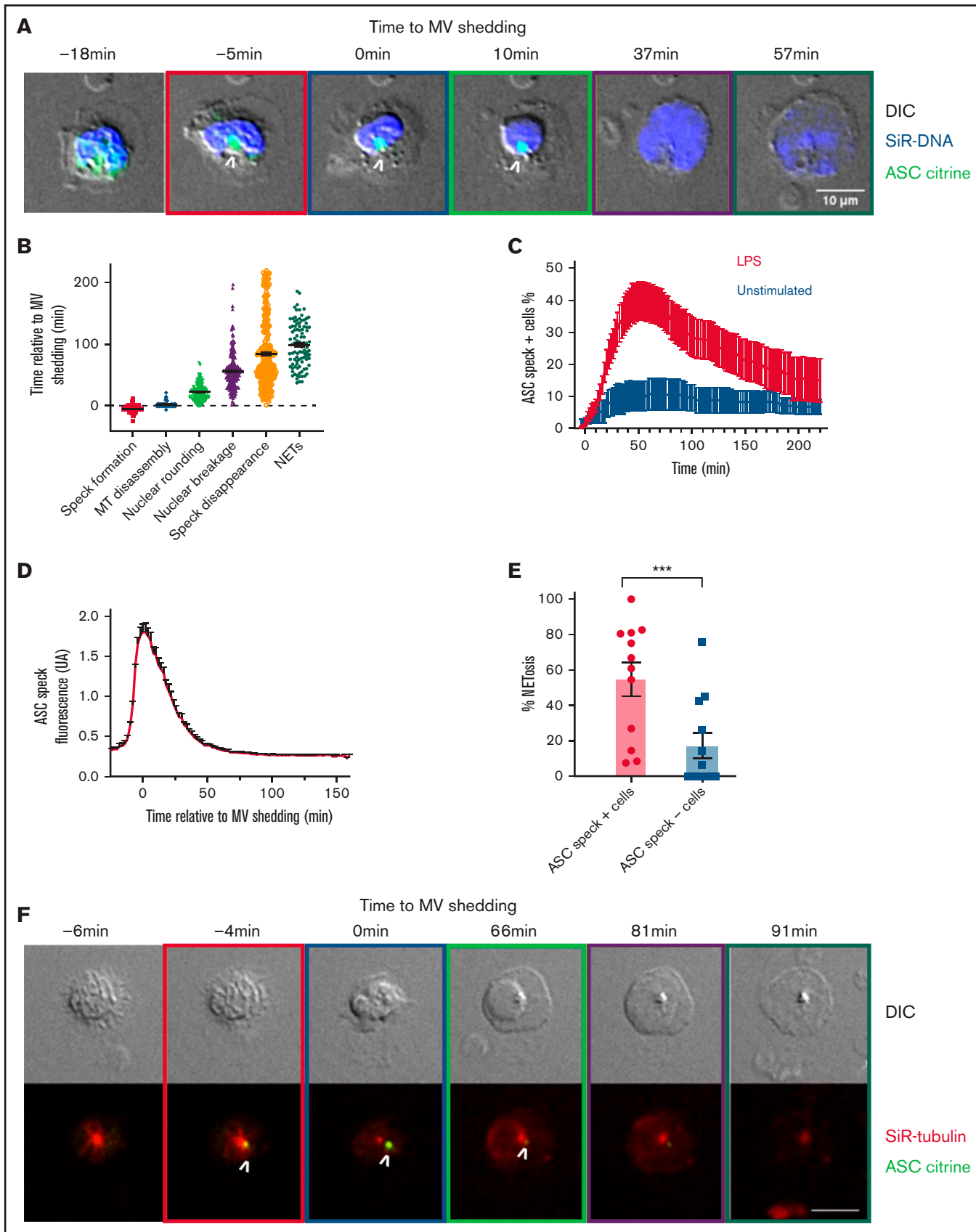


Figure 5.

speck is similar to that seen in mononuclear cells. Given their wide presence in the blood and lung compared with other types of leukocytes, we can conclude that neutrophils could be the major producers of specks. These findings support the possibility that both neutrophils and monocytes contribute to the cytokine storm through the inflammasome, and in vivo ASC speck detection could serve as an indicator of innate immune system activation. In bacterial sepsis, Cui et al has shown that assessing ASC speck-positive immune cells by flow cytometry could be used as a potential biomarker of patients at risk of death.<sup>25</sup>

Although the assembly of speck, which depends on the initial inflammasome polymerization, was obvious, we could not definitively determine which types of inflammasome were activated. Coimmunostaining of ASC and inflammasome sensors like AIM2, NLRP1, NLRC4, and NLRP3 showed that many of the ASC specks observed in COVID-19 neutrophils colocalized with NLRC4 or NLRP3 staining (supplemental Figure 2; supplemental Table 3). Interestingly, expression quantitative trait loci associated with higher expression of the 2 inflammasome genes NLRC4 and NLRP3 were also significantly linked to severe COVID-19 disease.<sup>26</sup> Under sterile inflammation, NLRP3 was the backbone of speck in murine neutrophils.<sup>10</sup> However, other inflammasome sensor components recently were seen in human neutrophils besides NLRP3.<sup>27-29</sup>

Interestingly, the genetic disorder due to a gain-of-function mutation in NLRP3 leading to excessive IL-1  $\beta$  production, called cryopyrin-associated periodic syndromes, has been described to be due mainly to neutrophil inflammasome activity and could be reproduced in mice by introducing the gain-of-function mutation only in neutrophils.<sup>30</sup> This shows that neutrophils with this mutation in NLRP3 represent the main cellular driver of cryopyrin-associated periodic syndromes and are an important source of IL-1 $\beta$ . This fits with our hypothesis that neutrophils substantially contribute to COVID-19 pathology.

The formation of speck occurred clearly in neutrophils with multilobular, nonrounding nuclei, indicating its assembly in the very early phases of NETosis. The early ASC speck formation suggests a possible role for caspase-1-mediated cleavage in cellular processes leading to NET release. In addition, caspase-1 activates formation of gasdermin D pores, important in both pyroptosis and NETosis.<sup>31-33</sup> Caspase-1 is known to have many substrates such as the cytoskeleton and nuclear envelop components that need to disassemble for NETosis to proceed,<sup>20</sup> and early caspase-1 activation could facilitate these processes. Notably MTs, a major component of cytoskeletal systems that are involved in the regulation and distribution of several cell organelles, are important for NET release.<sup>34,35</sup> The formation of speck preceding MT disassembly may be because

microtubule transport is needed for ASC protein assembly at the inflammasome.<sup>23,24,36</sup>

Interestingly, NETs bind on von Willebrand Factor (VWF).<sup>37</sup> We carefully analyzed VWF plasma levels and activity of ADAMTS13, its cleaving enzyme. VWF levels were high in all patients, with most exceeding 500% of the normal value (supplemental Table 1). This observed high-endothelial release of VWF may promote retention of NETs in the affected organs as VWF binds to NETs. The very high VWF/ADAMTS13 activity ratio is likely primarily due an incredible endothelial activation rather than low ADAMTS13 activity, as would be seen in thrombotic thrombocytopenic purpura. This is supporting the idea that COVID-19 is a disease primarily affecting endothelial, platelet, and neutrophil activation, thus easily resulting in thrombosis.<sup>9,38-41</sup>

The high level of citrullinated nuclei was correlated with the percentage of neutrophils presenting a speck. The discrepancy between percent of cell-forming speck and percent of cell with citrullinated nuclei could be explained by the fact that citrullination is an irreversible posttranslational modification as opposed to speck formation. Indeed, we showed that speck formation occurs transiently in murine neutrophils before nuclear decondensation. Our results are reinforced by recent studies suggesting a link between NETs and the presence of extracellular inflammasomes.<sup>42,43</sup> Chen et al showed via electron microscopy and immunofluorescence that inflammasome-signaling proteins like caspase-1 and ASC speck are present in NETs of human thrombi and associated with H3cit, the marker of NETosis.<sup>43</sup> The role of the NLRP3 inflammasome in thrombosis and NETosis in the development of deep vein thrombosis was also recently uncovered.<sup>10,42</sup> In these studies, pharmacological inhibition of caspase-1 or NLRP3 strongly reduced deep vein thrombosis in mice. These observations together with high VWF levels in the severe COVID-19 patients further emphasize the propensity for pathological thrombosis observed in COVID-19.

The single-cell analysis of the redistribution of ASC-citrine leading to speck formation in murine neutrophil revealed a rapid and dynamic cellular process. This rapid triggering of ASC speck formation generating a transient and spatially confined wave of inflammasome activity was also observed in the subcapsular macrophages of the lymph node on viral infection in vivo.<sup>44</sup> However, in COVID-19, speck formation is not restricted to lymph nodes. Activation of inflammasomes was observed in peripheral mononuclear cells and now by us in the most prominent white blood cell: the neutrophil. Together, this may explain the unusual cytokine storm described in the SARS-Cov-2 infection. The gradual disappearance of speck fluorescence observed in stimulated neutrophils may indicate either speck dissolution or ASC protein cleavage. The mechanism of ASC

**Figure 5. Inflammasome activation kinetics and localization during NETosis in mouse neutrophils.** ASC citrine (green) reporter neutrophils were stained with far-red SiR-DNA (blue) or with far-red SiR-tubulin (red), and time-lapse DIC and spinning-disk confocal images were taken at 2- to 5-minute intervals for 4 hours. (A) Time series of image overlays of DIC (grayscale) and fluorescence of cell and DNA dynamics in neutrophils during NETosis in the presence of LPS. (A and F) Boxes around images indicate different cellular events (orange, speck formation; purple, microvesicle shedding [MV]; green, nuclear rounding; yellow, DNA release to the cytosol; black, extracellular DNA release). (B) Timing of cellular events relative to MV shedding under LPS activation. Each dot represents an individual cell. (C) Arithmetic means of percentage of cells forming ASC speck as a function of time in the absence (black curve) or in presence (red curve) of LPS added at time = 0 minutes. (D) Fluorescence intensity of ASC-citrine speck in neutrophils according to the time relative to MV shedding. Values are means plus or minus SEM. (E) Percentage of NETosis in cells forming speck (●) or in cells not forming speck (■) under LPS stimulation. Each dot represents 1 independent experiment. Bar size represents the mean of 12 independent experiments. A Mann-Whitney *U* test was used; \*\*\**P* < .001. (F) Time series of image overlays of DIC (grayscale) and fluorescence of ASC (green) and MT (red) in mouse neutrophils. White arrows indicate the presence of the ASC speck. Scale bar, 10  $\mu$ m. MT, microtubules; SEM, standard error of the mean.

speck disassembly first detected in our study needs to be defined in future investigation.

In conclusion, our results showed that an aberrant inflammasome activation occurs in neutrophils under infectious conditions and might be damaging to the host. Targeting inflammasome in neutrophils may be a therapeutic target to reduce NETosis and restore homeostasis.

## Acknowledgments

The authors would like to thank their Dean, George Q. Daley, for his support of COVID-19 research at Harvard Medical School (HMS) and his encouragement for this particular clinical study. They also thank all the patients who have participated in this study and their families. The authors wish to thank the Marine Biological Laboratory (MBL) for support as Denisa Wagner is a part of the Whitman Center faculty. They want to thank Nikon Instruments, especially John Allen, for the loan of microscopy equipment at MBL and, in particular, Clare Waterman for her helpful discussions. They thank Douglas T. Golenbock for advice on the ASC-citrine transgenic mice. The authors also thank the Microscopy Resources on the North Quad (MicRoN) core at HMS and the meticulous proofreading of the manuscript by Casey Sheehy and Sarah Gutch. They thank Genentech for their financial support of patient charges.

P.M. received an Individual Marie Skłodowska-Curie Actions fellowship by the European Commission (796365 - COAGU-LANT). This work was supported by the National Institutes of Health (NIH)/Research Program Award grant R35 HL135765 (D.W.), by the NIH/National Heart, Lung, and Blood Institute grant T32 HL007633-35 (J.N.), and by the NIH/National Institute of Allergy and Infectious Diseases grant U01AI138318 (J.L. and M.P); by the Massachusetts Consortium on Pathogen Readiness

(MassCPR) Evergrande COVID-19 Response Fund Award to B.R.; and by a generous gift to D.W. from the Steven Berzin family.

## Authorship

Contribution: K.A., J.N., S.G., S.F., and P.M. designed and performed the experiments and analyzed the data; D.D.W. designed the study and supervised the research; L.E.F. recruited the patients, contributed to the experimental design, and proofread the manuscript; K.Z.-V. collected clinical samples and data; M.D., M.S., R.M.B., B.A.R., J.A.L., and M.A.P. contributed to the experimental design and proofread the manuscript; and K.A., J.N., and D.D.W. wrote the manuscript.

Conflict-of-interest disclosure: D.D.W. is on the Scientific Advisory Board of Neutrolis, a preclinical-stage biotech company focused on DNases, and is a consultant to Takeda, both unrelated to this project. L.E.F. reports prior clinical trial support from Asahi Kasei Pharma America and research funding to the institution from Bayer AG outside the submitted work. R.M.B. has served on advisory boards for Merck and Genentech for work unrelated to this manuscript. The remaining authors declare no competing financial interests.

ORCID profiles: K.A., 0000-0002-9587-8822; J.N., 0000-0003-0490-208X; L.E.F., 0000-0002-7447-6453; K.Z.-V., 0000-0003-1310-4901; S.G., 0000-0002-2615-8266; M.D., 0000-0003-4028-8507; B.A.R., 0000-0003-2206-5748; D.D.W., 0000-0002-4494-413X.

Correspondence: Denisa Wagner, Program in Cellular and Molecular Medicine, Boston Children's Hospital, 1 Blackfan Circle, 9th Floor, Boston, MA 02115; e-mail: denisa.wagner@childrens.harvard.edu.

## References

1. Chen N, Zhou M, Dong X, et al. Epidemiological and clinical characteristics of 99 cases of 2019 novel coronavirus pneumonia in Wuhan, China: a descriptive study. *Lancet*. 2020;395(10223):507-513.
2. Mehta P, McAuley DF, Brown M, Sanchez E, Tattersall RS, Manson JJ; HLH Across Speciality Collaboration, UK. COVID-19: consider cytokine storm syndromes and immunosuppression. *Lancet*. 2020;395(10229):1033-1034.
3. Conti P, Ronconi G, Caraffa A, et al. Induction of pro-inflammatory cytokines (IL-1 and IL-6) and lung inflammation by Coronavirus-19 (COVI-19 or SARS-CoV-2): anti-inflammatory strategies. *J Biol Regul Homeost Agents*. 2020;34(2):327-331.
4. He L, Ding Y, Zhang Q, et al. Expression of elevated levels of pro-inflammatory cytokines in SARS-CoV-infected ACE2+ cells in SARS patients: relation to the acute lung injury and pathogenesis of SARS. *J Pathol*. 2006;210(3):288-297.
5. Wen W, Su W, Tang H, et al. Immune cell profiling of COVID-19 patients in the recovery stage by single-cell sequencing [published correction appears in *Cell Discov*. 2020;6:41]. *Cell Discov*. 2020;6(1):31.
6. Ferreira AC, Soares VC, de Azevedo-Quintanilha IG, et al. SARS-CoV-2 engages inflammasome and pyroptosis in human primary monocytes [published correction appears in *Cell Death Discov*. 2021;7(1):116]. *Cell Death Discov*. 2021;7(1):43.
7. Rodrigues TS, de Sá KSG, Ishimoto AY, et al. Inflammasomes are activated in response to SARS-CoV-2 infection and are associated with COVID-19 severity in patients. *J Exp Med*. 2021;218(3):e20201707.
8. Stutz A, Horvath GL, Monks BG, Latz E. ASC speck formation as a readout for inflammasome activation. *Methods Mol Biol*. 2013;1040:91-101.
9. Sorvillo N, Cherpokova D, Martinod K, Wagner DD. Extracellular DNA NET-works with dire consequences for health. *Circ Res*. 2019;125(4):470-488.
10. Münzer P, Negro R, Fukui S, et al. NLRP3 inflammasome assembly in neutrophils is supported by PAD4 and promotes NETosis under sterile conditions. *Front Immunol*. 2021;12:683803.
11. Martinod K, Wagner DD. Thrombosis: tangled up in NETs. *Blood*. 2014;123(18):2768-2776.

12. Thomas GM, Carbo C, Curtis BR, et al. Extracellular DNA traps are associated with the pathogenesis of TRALI in humans and mice. *Blood*. 2012; 119(26):6335-6343.
13. Veras FP, Pontelli MC, Silva CM, et al. SARS-CoV-2-triggered neutrophil extracellular traps mediate COVID-19 pathology. *J Exp Med*. 2020; 217(12):e20201129.
14. Ma A, Cheng J, Yang J, Dong M, Liao X, Kang Y. Neutrophil-to-lymphocyte ratio as a predictive biomarker for moderate-severe ARDS in severe COVID-19 patients. *Crit Care*. 2020;24(1):288.
15. Middleton EA, He XY, Denorme F, et al. Neutrophil extracellular traps contribute to immunothrombosis in COVID-19 acute respiratory distress syndrome. *Blood*. 2020;136(10):1169-1179.
16. Linszen RS, Chai G, Ma J, et al. Neutrophil extracellular traps increase airway mucus viscoelasticity and slow mucus particle transit. *Am J Respir Cell Mol Biol*. 2021;64(1):69-78.
17. Hassani M, Hellebrekers P, Chen N, et al. On the origin of low-density neutrophils. *J Leukoc Biol*. 2020;107(5):809-818.
18. Schulte-Schrepping J, Reusch N, Paclik D, et al; Deutsche COVID-19 OMICS Initiative (DeCOI). Severe COVID-19 is marked by a dysregulated myeloid cell compartment. *Cell*. 2020;182(6):1419-1440.e23.
19. Sánchez-Cerrillo I, Landete P, Aldave B, et al; REINMUN-COVID and EDEPIMIC groups. COVID-19 severity associates with pulmonary redistribution of CD1c+ DCs and inflammatory transitional and nonclassical monocytes. *J Clin Invest*. 2020;130(12):6290-6300.
20. Thiam HR, Wong SL, Qiu R, et al. NETosis proceeds by cytoskeleton and endomembrane disassembly and PAD4-mediated chromatin decondensation and nuclear envelope rupture. *Proc Natl Acad Sci USA*. 2020;117(13):7326-7337.
21. Tzeng T-C, Schattgen S, Monks B, et al. A fluorescent reporter mouse for inflammasome assembly demonstrates an important role for cell-bound and free ASC specks during *in vivo* infection. *Cell Rep*. 2016;16(2):571-582.
22. Sun Z, Gong W, Zhang Y, Jia Z. Physiological and pathological roles of mammalian NEK7. *Front Physiol*. 2020;11:606996.
23. Li X, Thome S, Ma X, et al. MARK4 regulates NLRP3 positioning and inflammasome activation through a microtubule-dependent mechanism. *Nat Commun*. 2017;8(1):15986.
24. Magupalli VG, Negro R, Tian Y, et al. HDAC6 mediates an aggresome-like mechanism for NLRP3 and pyrin inflammasome activation. *Science*. 2020;369(6510):eaas8995.
25. Cui J, Oehrl S, Ahmad F, et al. Detection of *in vivo* inflammasome activation for predicting sepsis mortality. *Front Immunol*. 2021;11(3641):613745.
26. Junqueira C, Crespo Á, Ranjbar S, et al. SARS-CoV-2 infects blood monocytes to activate NLRP3 and AIM2 inflammasomes, pyroptosis and cytokine release. *medRxiv [Preprint]*. 2021.
27. Schroder K, Tschopp J. The inflammasomes. *Cell*. 2010;140(6):821-832.
28. Chen KW, Groß CJ, Sotomayor FV, et al. The neutrophil NLR4 inflammasome selectively promotes IL-1 $\beta$  maturation without pyroptosis during acute Salmonella challenge. *Cell Rep*. 2014;8(2):570-582.
29. Greaney AJ, Portley MK, O'Mard D, et al. Frontline Science: Anthrax lethal toxin-induced, NLRP1-mediated IL-1 $\beta$  release is a neutrophil and PAD4-dependent event. *J Leukoc Biol*. 2020;108(3):773-786.
30. Stackowicz J, Gaudenzio N, Serhan N, et al. Neutrophil-specific gain-of-function mutations in Nlrp3 promote development of cryopyrin-associated periodic syndrome. *J Exp Med*. 2021;218(10):e20201466.
31. Sollberger G, Choidas A, Burn GL, et al. Gasdermin D plays a vital role in the generation of neutrophil extracellular traps. *Sci Immunol*. 2018; 3(26):eaar6689.
32. Karmakar M, Minns M, Greenberg EN, et al. N-GSDMD trafficking to neutrophil organelles facilitates IL-1 $\beta$  release independently of plasma membrane pores and pyroptosis. *Nat Commun*. 2020;11(1):2212.
33. Chen KW, Monteleone M, Boucher D, et al. Noncanonical inflammasome signaling elicits gasdermin D-dependent neutrophil extracellular traps. *Sci Immunol*. 2018;3(26):eaar6676.
34. Neubert E, Meyer D, Rocca F, et al. Chromatin swelling drives neutrophil extracellular trap release. *Nat Commun*. 2018;9(1):3767.
35. Lai H-J, Hsu Y-H, Lee G-Y, Chiang H-S. Microtubule-mediated NLRP3 inflammasome activation is independent of microtubule-associated innate immune factor GEF-H1 in murine macrophages. *Int J Mol Sci*. 2020;21(4):1302.
36. Misawa T, Takahama M, Kozaki T, et al. Microtubule-driven spatial arrangement of mitochondria promotes activation of the NLRP3 inflammasome. *Nat Immunol*. 2013;14(5):454-460.
37. Fuchs TA, Brill A, Duerschmied D, et al. Extracellular DNA traps promote thrombosis. *Proc Natl Acad Sci USA*. 2010;107(36):15880-15885.
38. Mancini I, Baronciani L, Artoni A, et al. The ADAMTS13-von Willebrand factor axis in COVID-19 patients. *J Thromb Haemost*. 2021;19(2):513-521.
39. Manne BK, Denorme F, Middleton EA, et al. Platelet gene expression and function in patients with COVID-19. *Blood*. 2020;136(11):1317-1329.
40. Zaid Y, Puhm F, Allaey I, et al. Platelets can associate with SARS-Cov-2 RNA and are hyperactivated in COVID-19. *Circ Res*. 2020;127(11):1404-1418.
41. Caillon A, Trimaille A, Favre J, Jesel L, Morel O, Kauffenstein G. Role of neutrophils, platelets, and extracellular vesicles and their interactions in COVID-19-associated thrombopathy. *J Thromb Haemost*. 2022;20(1):17-31.

42. Campos J, Ponomaryov T, De Prendergast A, et al. Neutrophil extracellular traps and inflammasomes cooperatively promote venous thrombosis in mice. *Blood Adv.* 2021;5(9):2319-2324.
43. Chen SH, Scott XO, Ferrer Marcelo Y, et al. Netosis and inflammasomes in large vessel occlusion thrombi. *Front Pharmacol.* 2021;11:607287.
44. Sagoo P, Garcia Z, Breart B, et al. In vivo imaging of inflammasome activation reveals a subcapsular macrophage burst response that mobilizes innate and adaptive immunity. *Nat Med.* 2016;22(1):64-71.